# Magnetic properties of stage-1 $CoCl_2$-graphite intercalation compounds diluted with $MgCl_2$

J. T. Nicholls

*Department of Physics, Massachusetts Institute of Technology, Cambridge, Massachusetts 02139*

G. Dresselhaus

*Francis Bitter National Magnet Laboratory, Massachusetts Institute of Technology, Cambridge, Massachusetts 02139*

(Received 7 December 1989)

We report a detailed study of the dilution of the magnetic properties of stage-1 $CoCl_2$-graphite intercalation compounds (GIC's) with nonmagnetic $MgCl_2$. The substitution of magnetic ions by nonmagnetic ions reduces the three-dimensional antiferromagnetic ordering temperature $T_N$, and reduces the low-temperature transition field $H_t$ that is a measure of the antiferromagnetic interlayer coupling. The intercalate layer in the stage-1 $Co_xMg_{1-x}Cl_2$-GIC's fills only 85% of the available volume of the intercalate gallery. The extrapolated value of the Co concentration, $x_p=0.65$, at which $H_t$ and $T_N$ go to zero, suggests that the 15% concentration of voids is distributed randomly throughout the intercalate layer. It is proposed that for $x \geq 0.65$ there is a connected magnetic two-dimensional triangular lattice. Our indirect measurement of the in-plane intercalate distribution is in agreement with recent transmission electron microscopy studies that show there is a connected network of intercalate with a structural coherence length as large as 1 $\mu$m.

## I. INTRODUCTION

Recently, cation mixtures have been used as a means of varying the magnetic properties of magnetic graphite intercalation compounds (GIC's). For example, stage-2 $Co_xNi_{1-x}Cl_2$-GIC's have been synthesized and their magnetic properties were interpreted in terms of mixed in-plane exchange parameters.[1] Other studies have investigated the mixed spin anisotropies of stage-2 $Co_xFe_{1-x}Cl_2$-GIC's,[2] in the hope of seeing a transition from $XY$ ($x=1$) to Ising ($x=0$) spin behavior, such as is observed in the pristine $Co_xFe_{1-x}Cl_2$ system.[3] Other approaches that have been applied to change the magnetic properties of the $CoCl_2$-GIC's include bi-intercalation[4] and the application of pressure.[5]

In this study we have used a somewhat different approach in that we have diluted the magnetic properties of stage-1 $CoCl_2$-GIC's with nonmagnetic $MgCl_2$ to yield stage-1 $Co_xMg_{1-x}Cl_2$-GIC's. In our approach, the $Mg^{2+}$ ions are randomly substituted for the $Co^{2+}$ ions within each intercalate layer, while all the structural parameters remain constant. (Bi-intercalation compounds, where the distance between adjacent magnetic layers is increased by the introduction of additional nonmagnetic layers, cannot be regarded as a diluted magnetic system because the $c$-axis repeat distance is not preserved.) We believe that the magnetic properties of the $MgCl_2$-diluted stage-1 $CoCl_2$-GIC's are relatively easy to understand because the nature of the magnetic phase transitions with respect to temperature and applied magnetic field are well established for the pure stage-1 $CoCl_2$-GIC's.[6] Moreover, dilution is the simplest of the random mixing pro-

cesses and is well understood theoretically.[7] Throughout this paper we use the notation that $x$ is equal to the Co concentration, as adopted in the experimental study of pristine $Co_xMg_{1-x}Cl_2$.[8]

$MgCl_2$ was chosen as the diluent because it possesses structural properties similar to $CoCl_2$; both pristine chlorides have the $CdCl_2$ structure, and the size of the $Mg^{2+}$ ion (0.65 Å) is close to that of the $Co^{2+}$ ion (0.74 Å). In addition, $MgCl_2$ ($T_{mp}=714\,^\circ C$) and $CoCl_2$ ($T_{mp}=724\,^\circ C$) have very similar melting temperatures $T_{mp}$, and the two chlorides mix as solid solutions across the whole concentration range.[9,10] Although the synthesis of pure $MgCl_2$-GIC's has not been previously reported, we had no problem synthesizing a pure stage-1 compound. $CdCl_2$ was another metal dichloride that was considered as a possible diluent; however, the $Cd^{2+}$ ion (0.97 Å) is large and there is evidence that there are concentration inhomogeneities in pristine $Co_xCd_{1-x}Cl_2$.[10,11]

This paper is organized as follows. In Sec. II the synthesis and characterization of the $Co_xMg_{1-x}Cl_2$-GIC samples are described. The magnetic properties of pure stage-1 $CoCl_2$-GIC's are reviewed in Sec. III. The magnetic results for the $MgCl_2$-diluted $CoCl_2$-GIC's are reported in Sec. IV. The discussion and interpretation of these results, on the basis of dilution, are presented in Sec. V.

## II. SAMPLE PREPARATION AND CHARACTERIZATION

To prepare the $Co_xMg_{1-x}Cl_2$ starting material, pristine $CoCl_2$ and $MgCl_2$ (both 99.99% pure) were crushed

together in the moisture-free environment of a glove bag filled with argon. The relative amounts of each chloride were crudely estimated by eye, and the mixture was then loaded into a quartz glass reaction ampoule with the graphite pieces and three atmospheres of $Cl_2$. The ampoule was sealed and a single-zone intercalation reaction was carried out at 600 °C for 2 months. Our experience shows that, under similar reaction conditions, $MgCl_2$ is the more difficult chloride to intercalate into graphite. Therefore, it was expected that the concentration ratio of the pristine chlorides loaded into the reaction ampoule would differ from the ratio within the intercalate layer of the resulting GIC. For this reason, the concentrations of $Co^{2+}$ ($x$) and $Mg^{2+}$ ($1 - x$) ions were determined from the GIC samples themselves, as described below. No attempt was made to systematically investigate the effect of temperature and reaction time in the intercalation conditions.

The samples were first characterized by $(00\ell)$ x-ray diffraction scans. Figure 1 shows a $\theta$-$2\theta$ x-ray diffraction scan, using Cu $K\alpha$ radiation, for a stage-1 $Co_{0.77}Mg_{0.23}Cl_2$-GIC with a $c$-axis repeat distance calculated from the indexed $(00\ell)$ peak positions to be $I_c$=9.42 Å. The relative amounts of Co and Mg at different locations of a particular sample were accurately determined by electron microprobe measurements. The microprobe performs a chemical analysis over a region that is ~2 $\mu$m in diameter, a length larger than any expected domain size.[12] The quoted Co concentration $x$ is the average value of measurements over many different points of the sample. For different types of graphite host material, highly oriented pyrolytic graphite (HOPG), kish graphite, and natural graphite flakes in the same reaction ampoule, $x$ was found to vary by less than 3% of its average value. The point-to-point variation within one sample was also about 3%. The chemical analysis of the electron microprobe extends only ~2 $\mu$m below the GIC

surface. As a check of the sample homogeneity in the $z$ direction, we measured the [Co]/[Mg] ratio on the surface of an as-intercalated natural flake and found it to be the same (to within the quoted experimental error) as that measured on the surface of a freshly cleaved sample.

From weight uptake measurements it is possible to determine the chemical formula $C_nCo_xMg_{1-x}Cl_2$ of the GIC. If the incommensurate intercalate lattice completely fills the intercalate gallery between the graphite layers, then $n = 4.16$. Experimentally, the intercalate layer fills only $f$% of the available volume and $n$ is then given by $n = 416/f$. In Table I we show filling factors calculated in two ways: (1) no chlorine excess was assumed, and (2), that there is a 10% chlorine excess. In the first case, the measured filling factors are in the range 85–92 %, consistent with the claim[13] that stage-1 $CoCl_2$-GIC's with ~90% filling factors can be synthesized using high chlorine pressures and high intercalation temperatures. There is evidence from electronic properties (through measurements of the change in the Fermi energy $\Delta E_F$ due to charge transfer) and wet chemical analysis that there is a chlorine excess of ~10%. If this excess is taken into account, the original filling factors are suppressed slightly, but are still much higher than previously quoted values of $\approx$70% (see Ref. 14, and references contained therein). There are many possible errors that can make weight uptake measurements inaccurate, for example, the accumulation of unreacted chloride on the GIC surface or fracture of the sample during intercalation. From scanning electron microscopy images, there was no evidence for the presence of chloride on the surface of as-intercalated samples. In conclusion, we are confident that the observed filling factor is ~85% for all Co concentrations $0 \leq x \leq 1$.

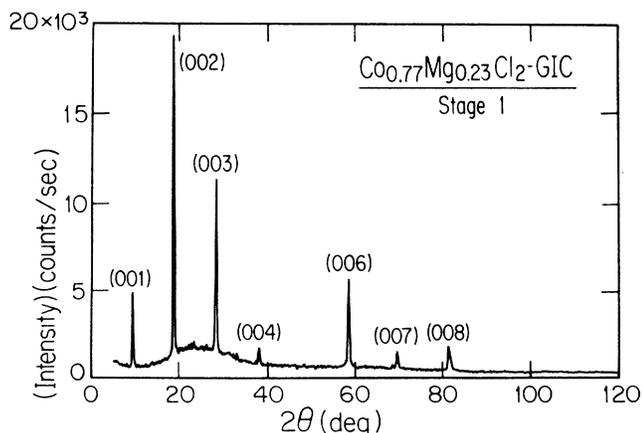In single-crystal stage-1 $MgCl_2$-GIC samples that were synthesized from natural graphite flakes, the $MgCl_2$ in-



FIG. 1. $(00\ell)$ x-ray diffraction scan of stage-1 $Co_{0.77}Mg_{0.23}Cl_2$-GIC. The $c$-axis repeat distance $I_c$=9.42 Å is calculated from the indexed peak positions.

TABLE I. Weight uptake percentages $W$ and calculated filling factors $f$ of stage-1 $Co_xMg_{1-x}Cl_2$-GIC samples.

| $x^a$ | $W^b$ (%) | (1) $f^c$ (%) | (2) $f^d$ (%) |
|---|---|---|---|
| 1.0 | 340 | 92 | 87 |
| 0.92 | 320 | 87 | 83 |
| 0.88 | 298 | 79 | 75 |
| 0.77 | 320 | 90 | 85 |
| 0.70 | 310 | 88 | 83 |
| 0.56 | 307 | 90 | 85 |
| 0.20 | 289 | 92 | 86 |
| 0.0 | 264 | 87 | 81 |

[a] Determined from electron microprobe measurements.
[b] $W$ denotes weight uptake defined by $W$=(weight of GIC)/(weight of host material).
[c] Filling factor $f$ calculated from GIC with formula $C_nCo_xMg_{1-x}Cl_2$.
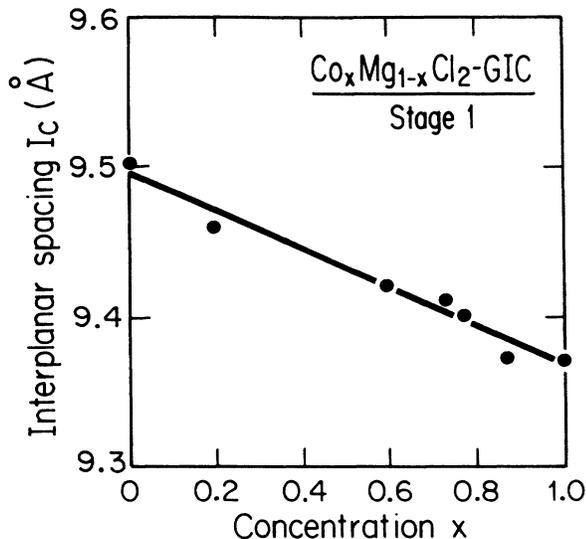[d] Filling factor $f$ calculated from GIC formula with a 10% chlorine excess $C_nCo_xMg_{1-x}Cl_{2.2}$.

FIG. 2. Intercalate $c$-axis repeat distance $I_c$ as a function of the $Co^{2+}$ concentration $x$ for the stage-1 random alloy $Co_xMg_{1-x}Cl_2$-GIC.

tercalate was found to form an incommensurate structure that exhibits rotational epitaxy, where the in-plane lattice vectors $a_{MgCl_2}$ and $a_{graphite}$ are aligned. The intercalate layers are stacked in an $\cdots \alpha\beta\gamma\alpha\beta\gamma\cdots$ sequence, similar to other stage-1 GIC's based on transition metal dichlorides of the $CdCl_2$ structure.[12,15] The $c$-axis repeat distance of the pure $MgCl_2$-GIC, $I_c$=9.50 Å, is in agreement with that obtained from inhomogeneous stage-1 $MgCl_2$ compounds.[16] In Fig. 2 we have plotted the $c$-axis repeat distance $I_c$ of the stage-1 $Co_xMg_{1-x}Cl_2$-GIC's as a function of the Co concentration $x$. Assuming that Vegard's law is valid we have least-squares fit the data with a straight line.

### III. PURE STAGE-1 CoCl$_2$-GIC's

It is advantageous to review the magnetic properties of pure stage-1 $CoCl_2$-GIC's, so that the effects of dilution with Mg can be better understood. The ac magnetic susceptibility $\chi = \chi' - i\chi''$, where $\chi'$ and $\chi''$ are the real and imaginary components, has been reported for the stage-1 $CoCl_2$-GIC's.[5] All information concerning the magnetic ordering can be obtained from $\chi'(H,T)$, where $H$ is an applied in-plane magnetic field.

The temperature-dependent susceptibility $\chi'(T)$ of stage-1 $CoCl_2$-GIC's shows two peaks; the upper peak has a maximum at $T_{max}$=9.7 K, and this temperature is identified to be the Néel temperature $T_N$. As the temperature is lowered through $T_N$, the ferromagnetically aligned spins within each magnetic layer become ordered into an antiferromagnetic arrangement along the $c$ axis. If the measurements of $\chi'(T)$ are repeated in an applied magnetic field $H$, the temperature where $\chi'(T)$ is a maximum $(T_{max})$ shifts to a lower temperature.

Low-temperature field sweeps of the in-plane susceptibility $\chi'(H)$ show a single field-induced peak[5] at the transition field $H_t$; in the limit $T \rightarrow 0$ K, $H_t$ approaches 380 Oe. As the temperature is increased, the field-induced structure at $H_t$ disappears about 0.2–0.3 K above $T_{max}$. $\chi'(H_t)$ shows the strongest peak susceptibility signal when the temperature is approximately $0.8T_N$. Earlier low-temperature measurements of $\chi'(H)$ for stage-1 $CoCl_2$-GIC's showed two field-induced transitions;[17] however, based on experience from measurements of many stage-1 $CoCl_2$-GIC samples, and the observation of similar effects in stage-1 $NiCl_2$-GIC's,[18] it is now believed that the transition at low fields is spurious and that high quality stage-1 samples show only one, clear, field-induced peak at $H_t$. We interpret $H_t$ to be the field value at which the antiferromagnetic interlayer coupling $J'$ is overcome. Neutron-scattering measurements confirm that there is a loss of antiferromagnetic order at $H_t$.[19]

In the next section we shall use the susceptibility methods described above to map out the corresponding $H_t$-$T$ phase diagrams for the stage-1 $Co_xMg_{1-x}Cl_2$-GIC's.

### IV. RESULTS FOR Mg-DOPED SAMPLES

In-plane ac susceptibility measurements of the magnetically diluted stage-1 $Co_xMg_{1-x}Cl_2$-GIC samples show a peak in $\chi'(T)$, similar to the case for $x$=1. The temperature of the susceptibility maximum $T_{max}$ decreases as the concentration of Mg ions increases. As an example, we show ac susceptibility results $\chi'(T)$ in Fig. 3(a) for a Co concentration of $x$=0.77, where the susceptibility maximum is at 3.7 K. In Fig. 3(b), we have plotted the value of $H_t(T)$ for the same sample, showing that the field-induced structure disappears at a temperature about 0.3 K above the peak position $T_{max}$ observed in
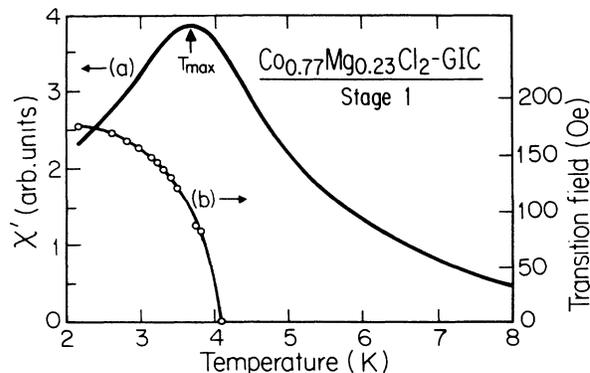


FIG. 3. The zero-field ac susceptibility $\chi'(T)$, labeled (a), of a HOPG-based stage-1 $Co_{0.77}Mg_{0.23}Cl_2$-GIC sample. The points, labeled (b), are the values of $H_t(T)$, showing that $H_t$ goes to zero about 0.3 K above the temperature of the susceptibility maximum $T_{max}$. The $H_t(T)$ data were obtained from the $\chi'(H)$ scans shown in Fig. 4.
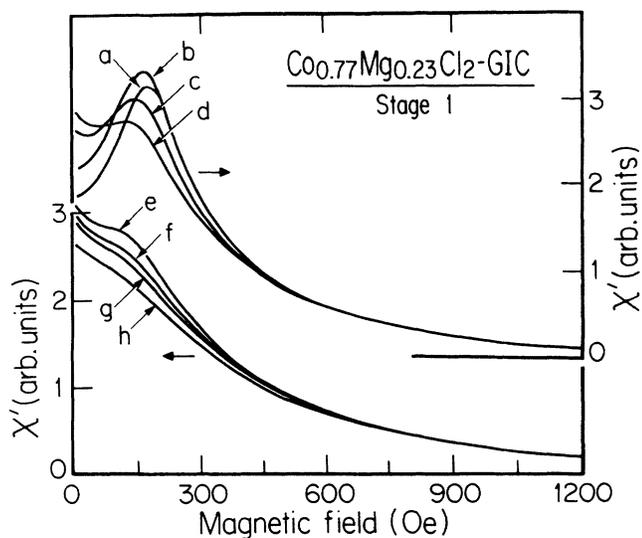
FIG. 4. Sweeps of $\chi'(H)$ for the sample $Co_{0.77}Mg_{0.23}Cl_2$-GIC at temperatures (a) 2.04, (b) 2.62, (c) 3.14, (d) 3.50, (e) 3.59, (f) 3.75, (g) 3.88, and (h) 4.14 K. The data are separated into two sets of four curves, both with the same scale, and offset from one another.



FIG. 6. The $H_t$-$T$ phase diagrams, derived from $\chi'(H)$ data, for stage-1 $Co_xMg_{1-x}Cl_2$-GIC's with concentrations (a) $x=1$, (b) $x=0.92$, (c) $x=0.88$, (d) $x=0.77$, and (e) $x=0.7$. The solid curves are a guide to the eye and the dashed curves are the expected extensions of the phase boundaries.

the corresponding temperature-dependent ac susceptibility $\chi'(T)$. The values of $H_t(T)$ [Fig. 3(b)] were derived from the field sweeps of $\chi'(H)$ shown in Fig. 4. For the concentration $x=0.77$, the low-temperature susceptibility $\chi'(H)$ curves are qualitatively similar to those of the pure stage-1 CoCl₂-GIC's, reviewed in Sec. III. There was no evidence of hysteresis in $\chi'(H)$ when the magnetic field was swept up and down.

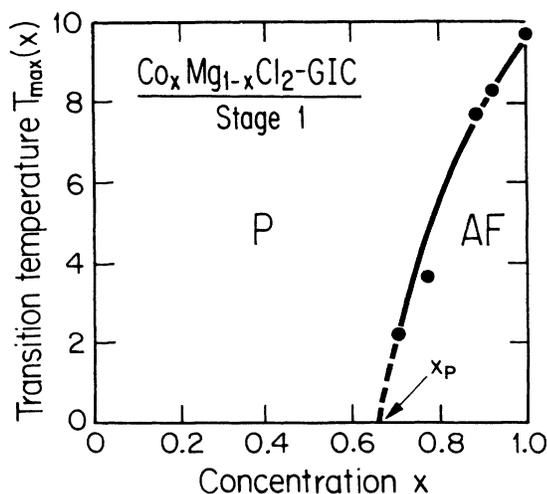The variation of the transition peak $T_{max}$ [see Fig. 3(a)] with Co concentration $x$ is plotted in Fig. 5. As $x$ de-

creases, the susceptibility peak broadens and the magnitude of the peak (in units of emu/mol Co²⁺) is reduced. This broadening effect makes it more difficult to accurately determine $T_{max}$ for samples with lower concentrations of Co²⁺ ions. For $x < 0.7$, the susceptibility peak is too low in temperature for us to measure in our present experimental set-up.

In Fig. 6 we present the $H_t$-$T$ phase diagrams, as determined from $\chi'(H)$ scans at constant temperature, for different Co concentrations. The values of the transition field $H_t$ extrapolated to zero temperature, and normal-



FIG. 5. The transition temperature $T_{max}$ of various stage-1 $Co_xMg_{1-x}Cl_2$-GIC's as a function of Co concentration $x$, showing the boundary between paramagnetic and antiferromagnetic behavior. The percolation threshold $x_p$ is noted.
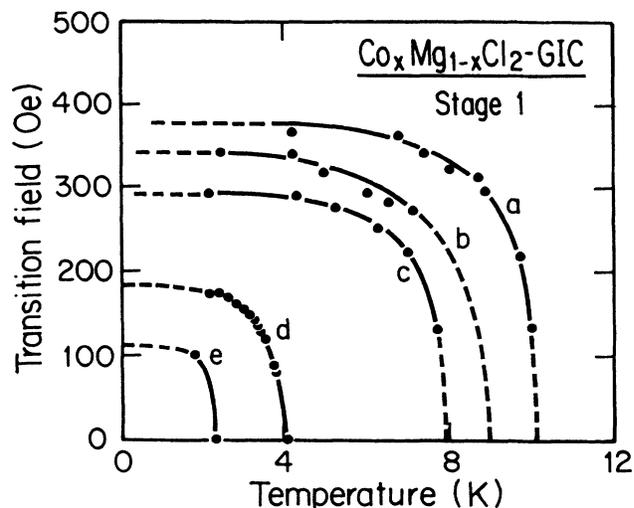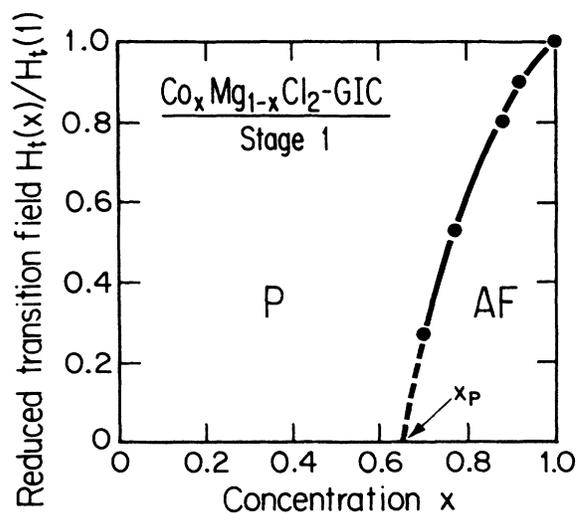


FIG. 7. Dependence on $x$ of the low-temperature transition field $H_t(x)$ of the stage-1 $Co_xMg_{1-x}Cl_2$-GIC's normalized by the undiluted value $H_t$ ($x = 1$) = 380 Oe.

ized by the undiluted value $H_t$=380 Oe, are plotted versus $x$ in Fig. 7. The effects of dilution on $H_t$ and $T_{max}$ shown in Figs. 5 and 7 look very similar, indicating that the reduction in the transition field $H_t$ scales with the reduction of the transition temperature $T_{max}$.

As previously mentioned, samples synthesized in the same reaction ampoule, but from different graphite host materials, have approximately the same Co concentrations. Further, measurements on those same GIC samples showed that they had identical magnetic properties.

In-plane resistivity measurements $\rho_a(T)$, see Fig. 8, were performed on a HOPG-based sample of Co concentration $x$=0.77. With decreasing temperature, $\rho_a(T)$ starts to rise at $T \approx 4$ K, close to the Néel temperature $T_N$ of the same sample as determined by the $\chi'(H)$ scans in Fig. 4. The magnetic scattering below $T_N$ gives rise to only a 1% increase in the magnitude of $\rho_a$.

High-field magnetization measurements of the doped GIC samples were carried out with the vibrating sample magnetometer that had been used in the study of the pure CoCl$_2$-GIC's.[20] In the magnetization experiment, the samples experience a very strong torque (**M × H**) when the magnetic field is applied along the hard direction, **H** ∥ $c$. To prevent the samples from rotating or cleaving, they were mounted in specially constructed Delrin sample cells containing an inert medium (Fluo-rinert made by 3M) that freezes the sample into a fixed position at low temperatures. The magnetization curves for a stage-1 Co$_{0.56}$Mg$_{0.44}$Cl$_2$-GIC sample at $T$=1.3 K are shown in Fig. 9 with the magnetic field **H** applied parallel ($M_\parallel$) and perpendicular ($M_\perp$) to the sample $c$ axis. Although this sample is not expected to exhibit antiferromagnetic order (see Figs. 5 and 7), the $g$ values, $g_\perp = 4.46$ (**H** ⊥ $c$ axis) and $g_\parallel = 3.30$ (**H** ∥ $c$ axis), determined from the saturation magnetization for the two



FIG. 9. The high-field magnetization parallel ($M_\parallel$) and perpendicular ($M_\perp$) to the $c$ axis of stage-1 Co$_{0.56}$Mg$_{0.44}$Cl$_2$-GIC at $T$=1.3 K.

configurations are anisotropic. A small amount of hysteresis was observed in the $c$-axis magnetization $M_\parallel(H)$ of samples with $x > 0.7$; these results are to be published elsewhere.[21]

## V. DISCUSSION

### A. The Hamiltonian and percolation

Pristine Co$_x$Mg$_{1-x}$Cl$_2$ exhibits magnetic behavior[8] that provides strong evidence that the two different cations distribute themselves randomly throughout the sample. We thus assume that the metal ions will also mix randomly in the stage-1 Co$_x$Mg$_{1-x}$Cl$_2$-GIC's. The similarity of the Mg$^{2+}$ and Co$^{2+}$ ion sizes leads us to believe that, in the diluted compounds, there will be little local distortion of the intercalate lattice, and that the remaining Co$^{2+}$-Co$^{2+}$ in-plane nearest-neighbor exchange interactions will be unperturbed. The Cl$^-$ ions about each Co$^{2+}$ ion should also remain arranged in the same octahedral configuration as in pristine CoCl$_2$; therefore, the point-group symmetry ($D_{3d}$) of the Co$^{2+}$ ion is retained. It has been experimentally observed[22] that the electronic energy levels of the Co$^{2+}$ ion are preserved when the ion is diluted in small concentrations (~5%) into MgCl$_2$. Therefore, the crystal-field theory of Lines,[23] developed for the Co$^{2+}$ ion in CoCl$_2$, should also be valid for the Co$^{2+}$ ion in the stage-1 Co$_x$Mg$_{1-x}$Cl$_2$-GIC's.

On the basis of the above symmetry arguments, we infer that the form of the Hamiltonian[24] used for the undiluted CoCl$_2$-GIC's,

$$\mathcal{H} = -J \sum_{i>j} \mathbf{S}_i \cdot \mathbf{S}_j + J_A \sum_{i>j} S_{iz} S_{jz} + J' \sum_{i>k} \mathbf{S}_i \cdot \mathbf{S}_k$$
$$-g_\perp \mu_B S H_6 \sum_i \cos(6\theta_i) \qquad (1)$$
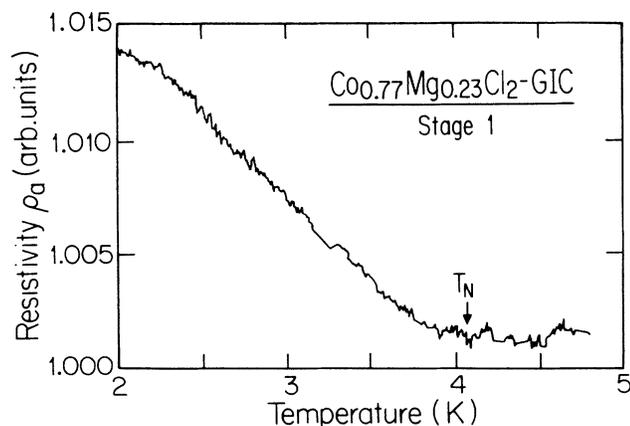


FIG. 8. Temperature dependence of the in-plane resistivity $\rho_a(T)$ of stage-1 Co$_{0.77}$Mg$_{0.23}$Cl$_2$-GIC showing an increase in resistivity as $T$ is lowered below $T \approx 4$ K, close to the Néel temperature $T_N$ of the same sample as determined by the $\chi'(H)$ scans in Fig. 4.
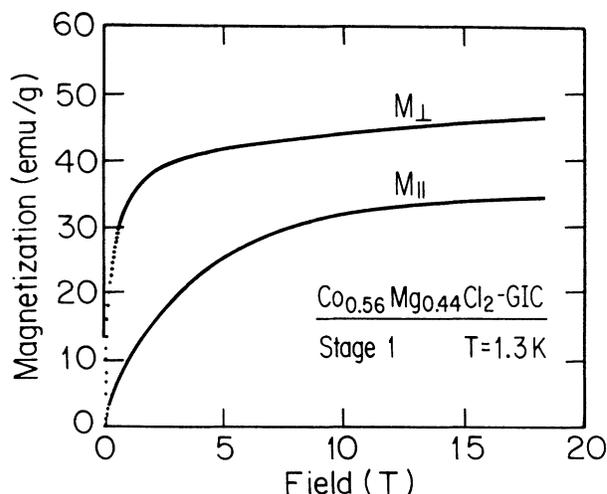
is also applicable to the diluted compounds. Upon dilution, the stage-1 CoCl₂-GIC values for the intraplanar ferromagnetic coupling $J$=28.5 K, and the interplanar antiferromagnetic coupling $J'$=0.025 K,[5] will be reduced due to a decrease in the number of Co²⁺ neighbors. The magnetization curves (see Fig. 9) show that, upon dilution, the $g$ values of the Co²⁺ ion remain anisotropic ($g_\perp > g_\parallel$), and that the magnetic spins lie down in the $XY$ plane.

Because of the similarity of the Co²⁺ and Mg²⁺ ions, the value of in-plane anisotropy field $H_6$, which is due to the electrostatic interaction of the Cl⁻ ions with the Co²⁺ ion, should remain unchanged by dilution. An increase of the resistivity $\rho_a(T)$ as $T$ is lowered below $T_N$ has been observed in measurements on stage-1 NiCl₂-GIC's (Ref. 25) and stage-1 CoCl₂-GIC's.[26] A possible theory to explain the anomalous increase in $\rho_a(T)$ below $T_N$ was proposed in the latter reference. The decrease in the size of the anomaly in $\rho_a$ at $T_N$, from 10% to 1% on dilution, is consistent with a decrease of $J'$ and a decrease in the low-temperature long-range $c$-axis antiferromagnetic order of the sample.

With the substitution of $1 - x$ magnetic ions by nonmagnetic ions, the transition temperature is expected to decrease linearly with $1 - x$ for small concentrations:

$$T_N(x)/T_N(1) = 1 - \alpha(1 - x) + \cdots . \qquad (2)$$

In mean-field theory the value $\alpha$=1 is predicted, but for layered magnetic systems there is theoretical and experimental evidence[27] that the value of $\alpha$ will be greater than unity. As the dilution is increased, the spins break up into connected clusters of spins, and the observed transition temperature will then deviate below the linear prediction of Eq. (2). Eventually, at a concentration just below the critical concentration $x_p$, the spin clusters are no longer connected and the spins within one cluster become uncorrelated with spins in another cluster. With the loss of long-range connectivity between clusters, the three-dimensional (3D) ordering temperature $T_N \rightarrow 0$ K as $x \rightarrow x_p$.

### B. Pristine Co$_x$Mg$_{1-x}$Cl₂

Before discussing the dilution properties of the stage-1 Co$_x$Mg$_{1-x}$Cl₂-GIC's we shall review the magnetic properties of the pristine Co$_x$Mg$_{1-x}$Cl₂ system. The saturation field $H_{\text{sat}}$, the applied in-plane magnetic field at which the antiferromagnetic interlayer coupling $J'$ is just overcome, has been measured for pristine Co$_x$Mg$_{1-x}$Cl₂ with electron spin resonance[8] at 4.2 K. The results[8] are plotted in Fig. 10 as a function of Co concentration $x$. Katsumata et al. concluded[8] from these results that $H_{\text{sat}} \rightarrow 0$ at the concentration $x \approx 0.3$, close to the critical percolation concentration $x_p$=0.2845 of a 2D triangular lattice with first- and second-nearest-neighbor in-plane exchange interactions. The authors suggest there is a second-nearest-neighbor antiferromagnetic coupling $J_2$, not written down in Eq. (1), that is in competition with
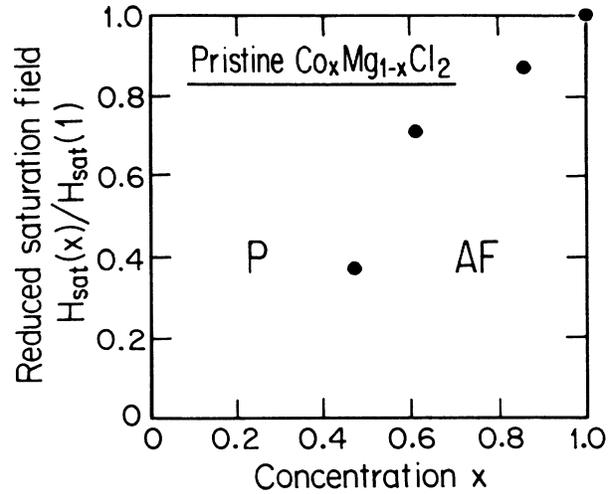


FIG. 10. Dependence on $x$ of the low-temperature saturation field $H_{\text{sat}}(x)$ of pristine Co$_x$Mg$_{1-x}$Cl₂ normalized by the undiluted value $H_{\text{sat}}$ ($x = 1$) = 32 kOe.[8]

the nearest-neighbor in-plane ferromagnetic coupling $J$, giving rise to 2D $XY$ spin-glass behavior. Although Hutchings[24] was not able to measure $J_2$, its existence is inferred from studies of other magnetic transition-metal dichlorides with the same structure. However, the interlayer-to-intralayer exchange coupling ratio of pristine CoCl₂ is $|J'/J| \sim 10^{-1}$, suggesting that the dilution properties of this system should be interpreted in terms of the percolation properties of the 3D lattice rather than the 2D lattice. Unfortunately, the percolation concentration for the CdCl₂ structure is not known, but another similarly connected lattice, the fcc structure, has a critical percolation concentration of $x_p$=0.195. In conclusion, we feel that the percolation concentration $x_p$ for the pure Co$_x$Mg$_{1-x}$Cl₂ system is not well determined experimentally (see Fig. 10), and from the well-studied 3D magnetic behavior of pristine CoCl₂ we expect the properties to be that of a diluted 3D magnetic system with a critical percolation concentration $x_p$ near 0.2.

### C. The stage-1 Co$_x$Mg$_{1-x}$Cl₂-GIC's

A full understanding of the magnetic properties of the stage-1 Co$_x$Mg$_{1-x}$Cl₂-GIC's requires detailed structural information. A typical (00$\ell$) x-ray diffraction scan (see Fig. 1) shows that the samples are well ordered in the out-of-plane $c$ direction. However, information from diffraction studies concerning the in-plane structure cannot distinguish the difference between the Fourier transform of an "island" distribution of intercalate from that of a "lake" distribution.[12] A number of length scales, obtained from different experiments on metal chloride GIC's all purport to be a measure of the in-plane structural coherence length within the intercalate layer. From small angle neutron-scattering scatter-

ing, Flandrois et al.[28] obtained an island size of $\sim$100 Å. A much larger length 900$\pm$150 Å was obtained from the upper bound of the in-plane spin correlation length in stage-2 $CoCl_2$-GIC measured using quasielastic neutron scattering.[29] The latter estimate may be affected by the large ($\sim$9°) mosaic spread of the sample. More recent information has been obtained by transmission electron microscopy (TEM) on stage-1 $CoCl_2$ samples made from fine graphite powder.[12] It is claimed that in these TEM images, free of moiré fringes, that the intercalate forms a connected network with an in-plane structural coherence length of $\sim$1 $\mu$m. Next we shall present arguments, from information obtained by diluting the magnetic $Co^{2+}$ lattice, that supports the claim that the intercalate forms a connected network.

The interlayer-to-intralayer exchange coupling ratio for the stage-1 $CoCl_2$-GIC's is $|J'/J| \sim 10^{-3}$, and hence the stage-1 $Co_xMg_{1-x}Cl_2$-GIC's (like other diluted quasi-2D magnetic systems, see Ref. 27) should have a percolation concentration $x_p$ determined by the 2D lattice of the layers that make up the 3D structure.

The pure stage-1 $CoCl_2$-GIC samples have an in-plane filling factor of 85%, and thus are already diluted by a 15% concentration of nonmagnetic impurities (voids). We shall assume that the in-plane voids in the "pure" stage-1 $CoCl_2$-GIC's are distributed randomly throughout the intercalate plane. The addition of more nonmagnetic impurities, in the form of $Mg^{2+}$ ions, is also expected to be random. If this is the case, then the results in Figs. 5 and 7 can be interpreted by shifting the concentration axis to the right by 0.15, relative to the data points. Therefore we can redefine $H_t(x) \rightarrow H_t(x^*)$ and $T_{max}(x) \rightarrow T_{max}(x^*)$, where $x^* = x - 0.15$. (We should also rescale the $y$-axis values, but this does not affect any of the subsequent conclusions.) This interpretation gives a percolation concentration of $x_p^* = x_p - 0.15 = 0.5$, equal to the theoretical percolation concentration for a 2D triangular lattice with only nearest-neighbor exchange interactions.[7] This is consistent with our original assumption that the voids and the $Mg^{2+}$ ions are randomly distributed throughout the intercalate layer. If the voids or the $Mg^{2+}$ ions were clustered, then the observed percolation concentration would have been upshifted from the theoretical value $x_p^* = 0.5$.

$CoCl_2$-GIC samples of the same nominal stage, and made by different research groups, may have different intercalate filling factors. Our results show (see Fig. 5) that this variation in the connectivity of the magnetic 2D lattice could account for the different transition temperatures observed by different research groups.

## VI. CONCLUSIONS

This is the first report of the synthesis and structure of the stage-1 $Co_xMg_{1-x}Cl_2$-GIC's. For all $x$ we measure the intercalate filling factor to be $\sim$85%. Using this new GIC system, we have performed the first study of the magnetic properties of a magnetic GIC as it is diluted in a controlled manner with a nonmagnetic species. The magnetic properties indicate that the $Mg^{2+}$ ions are randomly substituted for the $Co^{2+}$ ions within the intercalate layer. The magnetic quantities $T_N$ and $H_t$, characteristic of long-range 3D antiferromagnetic order, go to zero at $x_p = 0.65$. The recalculated percolation concentration ($x_p^* = x_p - 0.15 = 0.5$), that accounts for a 15% random distribution of voids, is equal to the percolation concentration of a 2D triangular lattice with only nearest-neighbor exchange interactions. This percolation result is consistent with a connected intercalate structure with a long in-plane structural coherence length, as recently observed by Speck et al.[12]

It would be of considerable interest to investigate the effect of dilution on the magnetic properties of stage-2 $CoCl_2$-GIC's, especially near the 2D transition temperature $T_{cu}$.

## ACKNOWLEDGMENTS

[1] M. Yeh, M. Suzuki, and C. R. Burr, Phys. Rev. B **40**, 1422 (1989).

[2] S. M. Sampere, L. J. Santodonato, M. Suzuki, and C. R. Burr, in *Extended Abstracts of the Materials Research Society Symposium on Graphite Intercalation Compounds*, edited by M. Endo, M. S. Dresselhaus, and G. Dresselhaus (MRS, Pittsburgh, PA, 1988), p. 81.

[3] P. Wong, P. M. Horn, R. J. Birgeneau, C. R. Safinya, and G. Shirane, Phys. Rev. Lett. **45**, 1974 (1980).

[4] I. Rosenman, F. Batallan, Ch. Simon, and L. Hachim, J. Phys. (Paris) **47**, 1221 (1986).

[5] J. T. Nicholls, C. Murayama, H. Takahashi, N. Mōri, T. Tamegai, Y. Iye, and G. Dresselhaus, Phys. Rev. B **41**, 4953 (1990).

[6] G. Dresselhaus, J. T. Nicholls, and M. S. Dresselhaus, *Graphite Intercalation Compounds II*, Vol. II of *Springer Series in Materials Science*, edited by H. Zabel and S.A. Solin (Springer-Verlag, Berlin, 1990).

[7] R. B. Stinchcombe, *Phase Transitions and Critical Phenomena*, edited by C. Domb and J. L. Lebowitz (Academic, London, 1983), Vol. 7, p. 151.

[8] K. Katsumata, S. Kawai, and J. Tuchendler, Solid State

Commun. **65**, 1211 (1988).

[9] A. Ferrari and A. Inganni, Atti Accad. Naz. Lincei Cl. Sci. Fis. [Series 6] **8**, 242 (1928).

[10] G. Garton and P. J. Walker, J. Cryst. Growth **33**, 331 (1976).

[11] M. C. K. Wiltshire, J. Phys. C **12**, 3571 (1979).

[12] J. S. Speck and M. S. Dresselhaus, Synth. Met. **34**, 211 (1989).

[13] G. Chouteau and R. Yazami, Europhys. Lett. **3**, 229 (1987).

[14] F. Baron, S. Flandrois, C. Hauw, and J. Gaultier, Solid State Commun. **42**, 759 (1982).

[15] J. S. Speck, J. T. Nicholls, B. J. Wuensch, J. M. Delgado, M. S. Dresselhaus, and H. Miyazaki (unpublished).

[16] E. Stumpp and A. Terlan, Carbon **14**, 89 (1976).

[17] K. Y. Szeto, S. T. Chen, and G. Dresselhaus, Phys. Rev. B **33**, 3453 (1986).

[18] J. T. Nicholls and G. Dresselhaus, Synth. Met. **34**, 519 (1989).

[19] G. Chouteau, J. Schweizer, F. Tasset, and R. Yazami, Synth. Met. **23**, 249 (1988).

[20] J. T. Nicholls, Y. Shapira, E. J. McNiff, Jr., and G. Dresselhaus, Synth. Met. **23**, 231 (1988).

[21] J. T. Nicholls, E. J. McNiff, Jr., and G. Dresselhaus (unpublished).

[22] G. D. Jones and C. W. Tomblin, Phys. Rev. B **18**, 5990 (1978).

[23] M. E. Lines, Phys. Rev. **131**, 546 (1963).

[24] M. T. Hutchings, J. Phys. C **6**, 3143 (1973).

[25] J. T. Nicholls, J. S. Speck, and G. Dresselhaus, Phys. Rev. B **39**, 10 047 (1989).

[26] K. Sugihara, N. C. Yeh, M. S. Dresselhaus, and G. Dresselhaus, Phys. Rev. B **39**, 4577 (1989).

[27] L. J. de Jongh, *Magnetic Phase Transitions*, Vol. 48 of *Springer Series in Solid-State Physics*, edited by M. Ausloos and R. J. Elliott. (Springer-Verlag, Berlin, 1983), p. 172.

[28] S. Flandrois, A. W. Hewat, C. Hauw, and R. H. Bragg, Synth. Met. **7**, 305 (1983).

[29] D. G. Wiesler and H. Zabel, Phys. Rev. B **36**, 7303 (1987).